Journal of Organometallic Chemistry 693 (2008) 3141–3150

Contents lists available at ScienceDirect

Journal of Organometallic Chemistry

journal homepage: www.elsevier.com/locate/jorganchem

Hydrogen-bonding network in new scorpionate-type ligand composed of pyridine/pyrrole hybrid and anion-binding behavior of the corresponding rhodium complexes in alkyne cyclotrimerization reaction

Motoki Toganoh, Naoyuki Harada, Hiroyuki Furuta *

Department of Chemistry and Biochemistry, Graduate School of Engineering, Kyushu University, 744 Moto-oka, Nishi-ku, Fukuoka 819-0395, Japan

ARTICLE INFO

Article history:
Received 12 May 2008
Received in revised form 1 July 2008
Accepted 3 July 2008
Available online 10 July 2008

Keywords:
Rhodium
Scorpionate ligand
Cyclotrimerization
Anion-binding

ABSTRACT

New heteroscorpionate ligands (**1** and **2**) having a di(pyridin-2-yl)(1*H*-pyrrol-2-yl)methane substructure are synthesized. X-ray crystallographic analysis on **1** and **2** reveals that they form unique hydrogen bonding networks depending on the size of neighboring groups in solid states. **1** and **2** can form cationic rhodium(I) complexes, wherein the counter anions form hydrogen bondings with the pyrrolic NH moiety. In alkyne cyclotrimerization reactions using those complexes as catalyst, the catalytic activity is significantly enhanced when electron-donating counter anions is placed near the metal center.

1. Introduction

Monoanionic tripodal nitrogen donor ligands such as tris(pyrazolyl)borate are isoelectronic with the cyclopentadienyl ligand and widely employed in coordination chemistry and catalyst [1,2]. They have been commonly used as supporting ligands, which enable isolation of structurally as well as electronically interesting transition metal complexes [3]. Unique asymmetrical monoanionic tripodal ligands based on tetrapyrrolic units have been developed recently and applied for catalyst and stabilization of high oxidation state of the metal center [4]. Alternatively, heteroscorpionate ligands and related compounds including functionalized bis(pyrazol-1-yl)methane are also studied extensively because of their high flexibility on metal coordination [5–8].

We are currently interested in hydrogen bonding networks as well as anion-bindings by pyrrolic NH moieties [9]. Such anion recognition has been applied to the controlling redox or photophysical properties [10], construction of supramolecules [11], and so on. In particular, anion effects on the reactions catalyzed by cationic metal complexes have gathered much attention, because such strategy does not require tedious chemical transformations for modification of catalysts and, consequently, has hopeful prospect in the field of catalysis [12,13]. For instance, significant refinement of reactivity is observed in the rhodium catalyzed hydroamination reactions [14], aldol reactions [15], and intramolecular cyclization reactions [16] through the anion exchange of the catalysts. Nevertheless, detailed research, especially from the viewpoint of coordination chemistry, has not enough pursued yet.

This time, a connection of different metal coordination sites like pyridine and pyrrole [17] was studied to produce new heteroscorpionate ligands (**1** and **2**, Chart 1), which showed unique hydrogen-bonding networks depending on the size of neighboring groups. Beside, rhodium(I) complexes bearing a variety of counter anions were prepared with those ligands and alkyne cyclotrimerization reactions [18] were carried out with those complexes. The reactivity is significantly dependent on counter anions and the result affords fundamental information about the anion effect on alkyne cyclotrimerization reactions.

2. Results and discussion

The new monoanionic tripodal nitrogen donor ligands (**1** and **2**) composed of two pyridine units and one pyrrole unit can be prepared easily as follows (Scheme 1). The ligand **1a** was synthesized from 2,2'-dipyridylketone (**3**) and pyrrole. Upon treatment of **3** in pyrrole with trifluoroacetic acid (TFA) at ambient temperature, addition reaction proceeded smoothly to give **1a** in 67% yield. Since *N*-substitution competes against *O*-substitution in alkylation reactions of **1a** with alkyl halides, chemical transformation from **1a** to **1b**,**c** is so far ineffective. Then, preparation of **1b**,**c** was achieved through protection of the pyrrole moiety. First, *N*-BOC-2-bromopyrrole (**4**, BOC = *t*-butoxycarbonyl), prepared as reported, was lithiated with *n*-BuLi at −78 °C [19]. Second, **3** was added to the

* Corresponding author.
E-mail address: hfuruta@cstf.kyushu-u.ac.jp (H. Furuta).

0022-328X/$ - see front matter © 2008 Elsevier B.V. All rights reserved.
doi:10.1016/j.jorganchem.2008.07.005

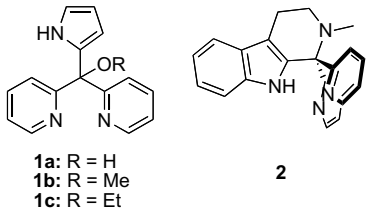

Chart 1. Structures of new scorpionate-type ligands.

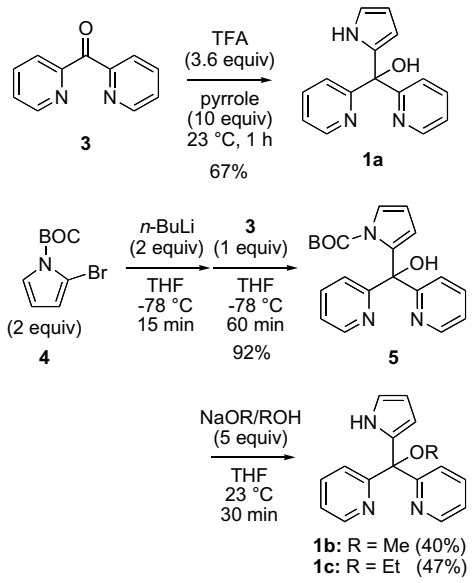

Scheme 1. Preparation of **1a**–**c**.

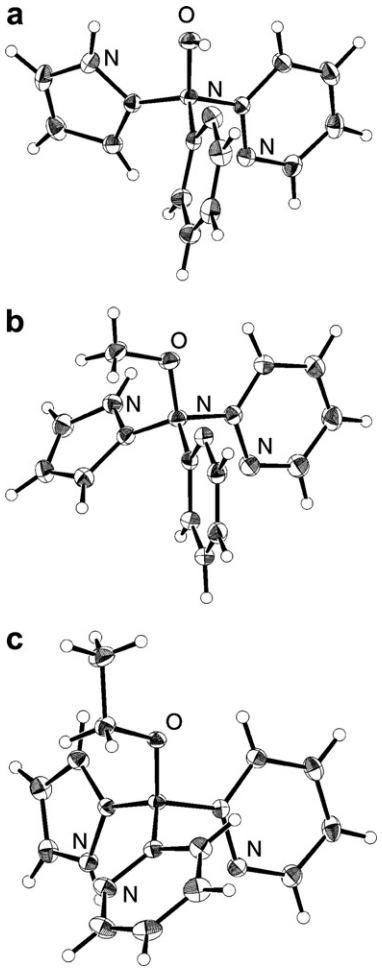

Fig. 1. Crystal structures of: (a) **1a**, (b) **1b**, and (c) **1c**. Thermal ellipsoids are shown at the 30% probability level.

resulting *N*-BOC-2-lithiopyrrole to give a carbinol (**5**) in 92% yield. **5** can be prepared by protection of **1a** albeit in much lower yield. Finally, treatment of **5** with NaOMe or NaOEt afforded **1b** or **1c** in 40% or 47% yield, respectively [20]. The ligand **2** was prepared via Pictet–Spengler reaction (Scheme 2) [21,22]. Heating of **3** and tryptamine (**6**) in the presence of *p*-toluenesulfonic acid (TsOH) gave the adduct **7** in 78% yield. Subsequent treatment of **7** with MeI under basic conditions afforded **2** in 99% yield [23]. The expeditious routes developed here allow us to obtain **1** and **2** in gram scales within a few days.

The structures of **1** and **2** are elucidated by X-ray crystallographic analysis. The ORTEP drawings of **1a**–**c** are shown in Fig. 1. The bis(2-pyridyl)pyrrolylmethane substructures are clearly observed in **1a**–**c**. Directions of the pyrrole rings as well as the pyridine rings differ in each molecule, indicating flexible rotation of these rings. Fig. 2 shows the X-ray structure of **2**. Compared to **1**, **2** has the rigid structure due to bridging between the indole moiety and the bis(2-pyridyl)methane moiety and hence the direction of NH moiety relative to the two pyridine rings is nearly fixed.

Because **1** and **2** have the hydrogen-donating pyrrole ring and the hydrogen-accepting pyridine ring in addition to the hydroxy or alkoxy groups, they form ordered architectures through hydro-

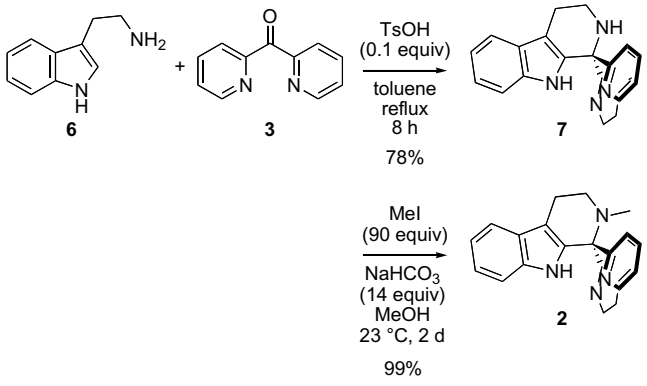

Scheme 2. Preparation of **2**.

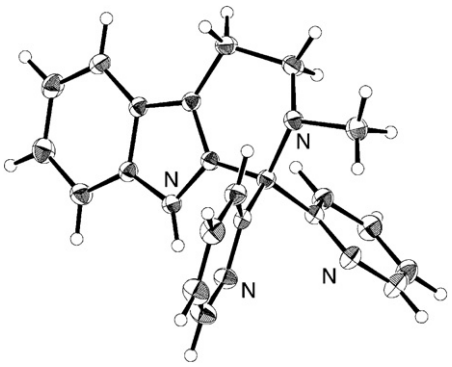

Fig. 2. Crystal structure of **2**. Thermal ellipsoids are shown at the 30% probability level.

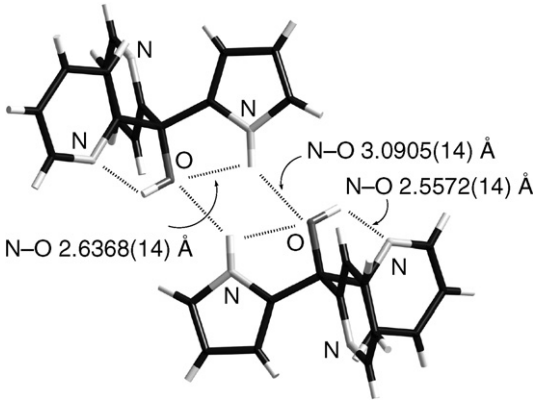

Fig. 3. Hydrogen-bonding network of **1a** in solid state.

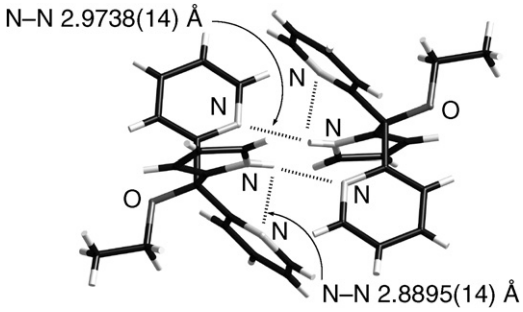

Fig. 5. Hydrogen-bonding network of **1c** in solid state.

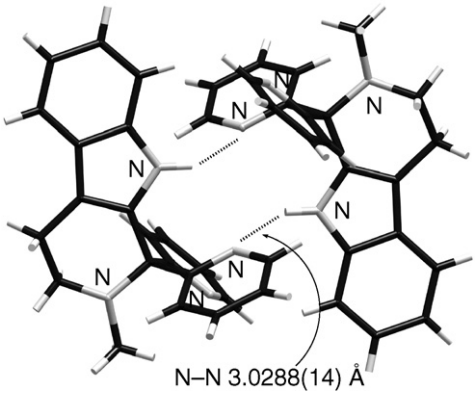

Fig. 6. Hydrogen-bonding network of **2** in solid state.

gen bondings in solid states. In the case of **1a**, formation of a dimeric structure is found as shown in Fig. 3. Intermolecular hydrogen bonding is formed between the pyrrolic NH moiety of one molecule and the oxygen atom of the adjacent molecule. The intermolecular N–O bond length is 3.0905(14) Å. The intramolecular NH–O bond (N–O bond length: 2.6368(14) Å) and the intramolecular OH–N bond (N–O bond length: 2.5572(14) Å) are also observed in **1a**. When the methyl group is introduced to the hydroxy moiety of **1a**, hydrogen bondings around this moiety are disturbed and 1D chain hydrogen-bonding network is constructed as illustrated with **1b** (Fig. 4). In **1b**, the methoxy group is not engaged for hydrogen bondings. Alternatively, sequential NH–N hydrogen bonds (N–N bond length: 3.1051(18) Å) are formed to construct zigzag alignments. Interestingly, this 1D chain network is easily torn into dimers by changing the methoxy group to the ethoxy group. In the solid state structure of **1c**, only a dimeric architecture is observed (Fig. 5) and no 1D chain networks are found at all. The oxygen atom does not contribute to hydrogen bondings and only intra- and intermolecular NH–N bonds (N–N bond lengths: 2.8895(14) and 2.9738(14) Å) are detected. Possibly due to different configuration derived from hydrogen bonding network, **1a**–**c** have totally different crystal systems (**1a**: monoclinic, **1b**: orthorhombic, **1c**: triclinic), although they do not contain any solvent molecules. In the case of **2**, only intermolecular NH–N bonds (N–N bond length: 3.0288(14) Å), which result in a formation of dimer, are observed (Fig. 6).

The cationic rhodium complexes **8a**-**Cl**, **8b**-**Cl**, and **9**-**Cl** are readily prepared by treatment of **1** and **2** with $[RhCl(cod)]_2$ (cod = 1,5-cyclooctadiene) at ambient temperature (Scheme 3). When **1a** was treated with $[RhCl(cod)]_2$ in CH_2Cl_2, coordination of **1a** to a rhodium metal proceeded smoothly to give the rhodium(I) complex **8a**-**Cl** in 95% yield. Similarly, treatment of **1b** afforded **8b**-**Cl** in 95% yield. The reaction of **2** with $[RhCl(cod)]_2$ also afforded the corresponding rhodium complex **9**-**Cl** in 95% yield. In the ^1H NMR spectra, the signals ascribable to the pyrrolic NH moieties are observed at δ 11.03 ppm for **8a**-**Cl**, 11.65 ppm for **8b**-**Cl**, and 13.43 ppm for **9**-**Cl**. Such significant low-field shifts from those of the intact ligands **1** and **2** (δ 9.41 ppm (**1a**), 10.78 ppm (**1b**), and 8.94 ppm (**2**)) suggest the existence of hydrogen bondings between the pyrrole NH moieties and the chloride anions [24].

Strong evidence for the structural assignment of the rhodium complexes is derived from the X-ray crystallographic analysis on **8a**-**Cl**. The ORTEP drawing of **8a**-**Cl** is shown in Fig. 7 and the selected structural parameters are listed in Table 1. The rhodium metal is coordinated by the two pyridine nitrogen atoms as well as the cod ligand. The distance between the chloride anion and the pyrrole nitrogen atom or the hydroxyl oxygen atom is 3.322(3) or 3.031(2) Å, respectively. These values show that the chloride anion is recognized by both the NH and OH moieties. While **8a**-**Cl** formally has the C_s symmetric structure, the bond lengths and the bond angles around the metal center are asymmetrical in solid

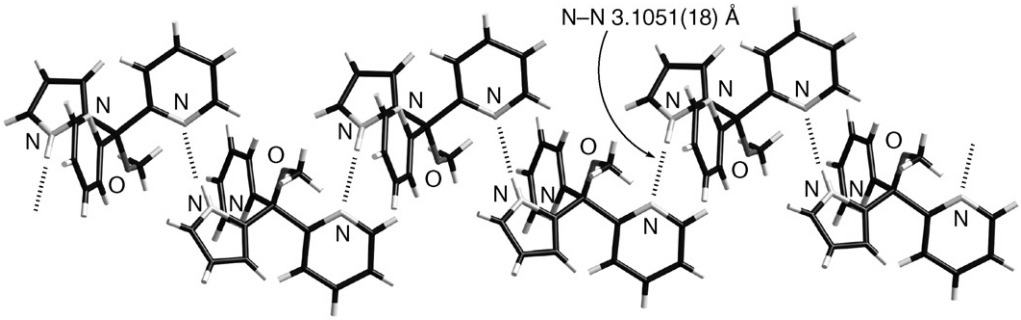

Fig. 4. Hydrogen-bonding 1D chain network of **1b** in solid state.

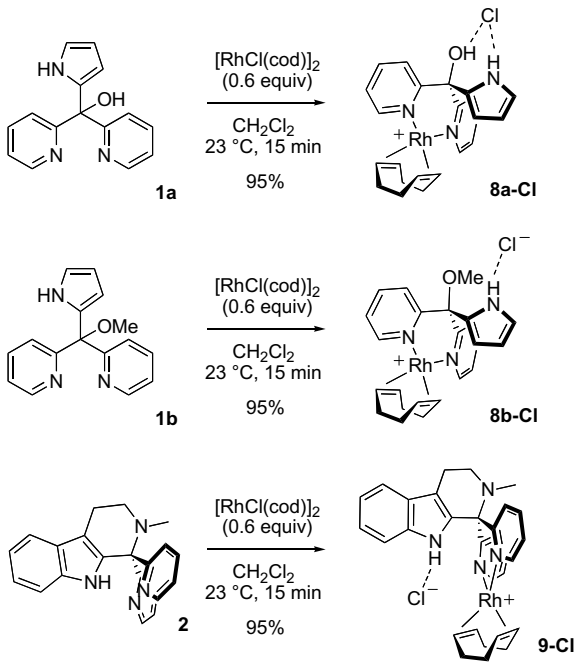

Scheme 3. Rhodium metalation of **1** and **2**.

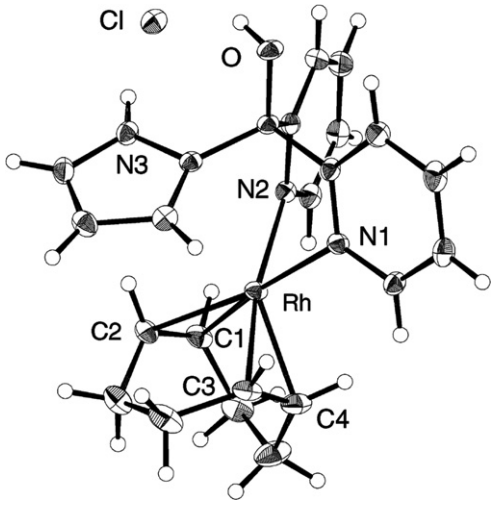

Fig. 7. Crystal structure of **8a-Cl**. Thermal ellipsoids are shown at the 30% probability level.

Table 1
Selected bond lengths (Å) and angles (°) for the X-ray structure of **8a-Cl**

Rh–C1	2.160(3)	C1–C2	1.389(4)
Rh–C2	2.143(2)	C3–C4	1.406(5)
Rh–C3	2.100(3)	∠N1–Rh–N2	82.60(8)
Rh–C4	2.092(4)	∠C1–Rh–C2	37.7(1)
Rh–N1	2.117(2)	∠C2–Rh–C3	81.2(1)
Rh–N2	2.177(2)	∠C3–Rh–C4	39.2(1)
O–Cl	3.031(2)	∠C4–Rh–C1	81.0(1)
N3–Cl	3.320(3)		

state. For example the Rh–N1 bond length (2.117(2) Å) is shorter than the Rh–N2 bond length (2.177(2) Å) by 0.06 Å.

Treatment of **8b-Cl** or **9-Cl** with $NaHCO_3$ resulted in the coordination of anionic pyrrole nitrogen atom through a loss of the HCl molecule as well as decoordination of one pyridine ligand to give neutral complexes **10b** or **11**, respectively (Scheme 4) [25]. Furthermore, treatment of **10b** or **11** with NH_4Cl caused regeneration of **8b-Cl** or **9-Cl**. These cycles are essentially reversible and interchange between the pyrrole ring and the pyridine ring occurs without decomposition of the complexes. In **10b** and **11**, a loss of hydrogen atom attached to the pyrrole nitrogen atom is surely confirmed by the ^{1}H NMR spectra and the detailed structure of **11** is elucidated by X-ray crystallographic analysis (Fig. 8 and Table 2). The anionic pyrrole nitrogen atom (N3) and one of the two pyridine nitrogen atoms (N1) coordinate to the metal center and another pyridine nitrogen atom (N2) remains free.

Manipulation of anions in **8a-Cl** and **9-Cl** is achieved in a common manner (Scheme 5). Anion exchange is possible by treatment with silver salts or sodium salts. For example, mixing of **8a-Cl** with $AgPF_6$ and subsequent recrystallization affords **8a-PF$_6$**. In a similar manner, the reactions of **9-Cl** with the corresponding silver salts give **9-PF$_6$**, **9-NO$_3$**, and **9-OCOCF$_3$**. In addition, treatment of **9-Cl** with $NaBPh_4$ gives **9-BPh$_4$**. The ^{1}H NMR signals of pyrrolic NH protons give definite information on the structures of the anion-exchanged rhodium complexes. The exchange of anions from chloride to hexafluorophosphate causes the high-field shifts (δ 9.28 ppm (**8a-PF$_6$**) and 11.71 ppm (**9-PF$_6$**)), which suggests weaker interaction between the NH moieties and the anions. While distinct anion bindings are implied for **9-NO$_3$** (δ 12.90 ppm) and **9-OCOCF$_3$** (δ 12.72 ppm), almost no interaction between the NH moiety and the anion is recognized in **9-BPh$_4$** (δ7.95 ppm).

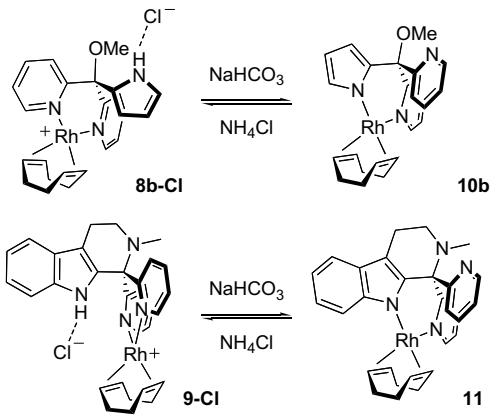

Scheme 4. Reversible interchange of the pyridine rings and the pyrrolic ring.

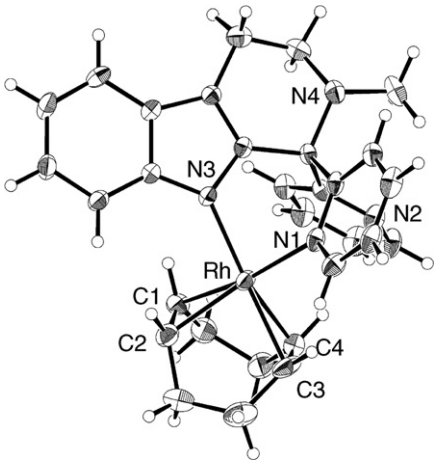

Fig. 8. Crystal structure of **11**. Thermal ellipsoids are shown at the 30% probability level.

Table 2
Selected bond lengths (Å) and angles (°) for the X-ray structure of **11**

Rh–C1	2.109(5)	C3–C4	1.350(8)
Rh–C2	2.153(5)	∠N1–Rh–N3	81.29(14)
Rh–C3	2.141(5)	∠C1–Rh–C2	37.0(2)
Rh–C4	2.134(5)	∠C2–Rh–C3	80.6(2)
Rh–N1	2.116(4)	∠C3–Rh–C4	36.8(2)
Rh–N3	2.076(4)	∠C4–Rh–C1	82.0(3)
C1–C2	1.353(8)		

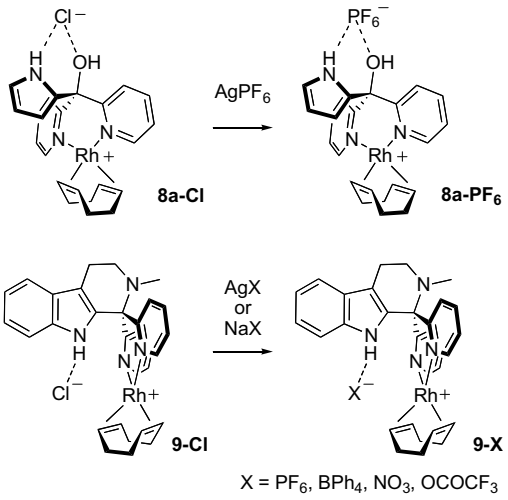

Scheme 5. Manipulation of anion in the anion-recognizing rhodium complexes.

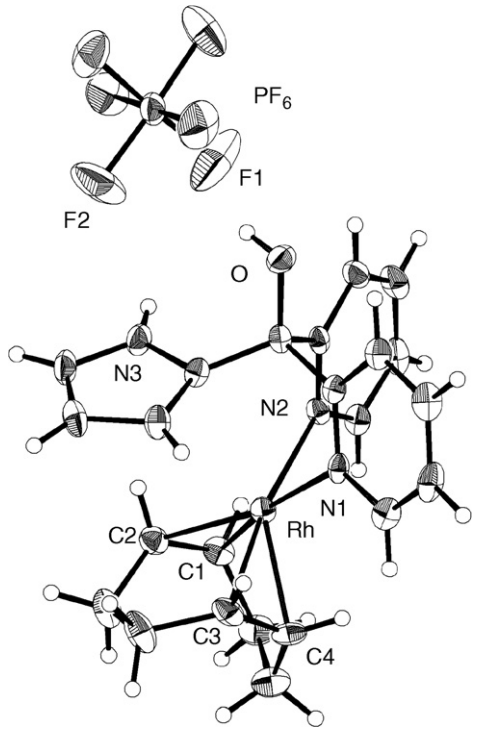

Fig. 9. Crystal structure of **8a**-PF_6. Thermal ellipsoids are shown at the 30% probability level.

Evidence for the structure of **8a**-PF_6 is obtained from X-ray crystallographic analyses. The ORTEP drawing of **8a**-PF_6 is shown in Fig. 9 and the selected structural parameters are summarized in Table 3. The structure of **8a**-PF_6 is similar to that of **8a**-**Cl**. For example, the Rh–N1 bond length (2.137(7) Å) and the Rh-N2 bond length (2.201(7) Å) differ significantly although it is C_s symmetric formally. The hexafluorophosphate ion is also recognized by both the NH and OH moieties. The shortest N3–F and the O–F bond lengths are 2.969(13) and 3.012(11) Å, respectively.

Table 3
Selected bond lengths (Å) and angles (°) for the X-ray structure of **8a**-PF_6

Rh–C1	2.172(9)	C1–C2	1.408(15)
Rh–C2	2.169(10)	C3–C4	1.426(15)
Rh–C3	2.133(9)	∠N1–Rh–N2	82.5(3)
Rh–C4	2.136(9)	∠C1–Rh–C2	37.8(4)
Rh–N1	2.137(7)	∠C2–Rh–C3	80.6(4)
Rh–N2	2.201(7)	∠C3–Rh–C4	39.0(4)
O–F1	3.012(11)	∠C4–Rh–C1	81.1(4)
N3–F2	2.969(13)		

With a variety of rhodium complexes in hands, anion effect in cyclotrimerization reactions of dimethyl acetylenedicarboxylate (DMAD) was investigated. A solution of DMAD in toluene or chlorobenzene was heated at 80 °C for 1 d in the presence of 1 mol% of the catalyst. The non-coordinative solvents would be important for the efficient cyclotrimerization, because no reaction proceeded when the reactions were carried out in THF at the refluxed temperature. The lower reaction temperature and the less amount of catalyst were adopted to establish anion effect, while the quantitative yields were obtained under the harsh conditions. The reactions proceeded cleanly and only the starting material and the product except for the catalysts were detected by ^{1}H NMR analysis after heating. The results are summarized in Table 4. The reactions with **8a**-**Cl** and **8b**-**Cl** essentially give the same results (21% yields), indicating both of the complexes take the similar structures in solution (entries 1 and 3). The use of **8a**-PF_6 affords the similar result (16% yield, entry 2). The solid phase structures of **8a**-**Cl** and **8a**-PF_6 suggest that the counter anions are placed on the opposite side of the ligands with the metal ions. Hence, the difference of the anions would not affect the reactions. Meanwhile, in the case of the reactions with **9**-**X**, where the anions would be placed on the same side with the metal center, considerable anion effect is observed in the alkyne cyclotrimerization reactions. Study on the anion effect with **9**-**X** is performed in chlorobenzene because of poor solubility of the catalysts in toluene. Note that the reactivity in chlorobenzene is

Table 4
Rhodium catalyzed cyclotrimerization reactions of DMAD

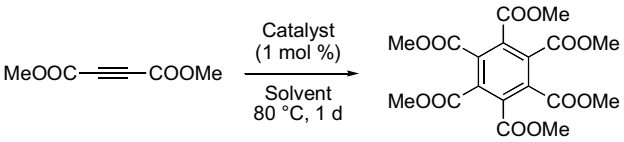

Entry	Catalyst	Solvent	Yield (%)	δ (ppm)[a]
1	**8a**-**Cl**	Toluene	21	11.03
2	**8a**-PF_6	Toluene	16	9.28
3	**8b**-**Cl**	Toluene	21	11.65
4	**9**-**Cl**	Toluene	54	13.43
5	**9**-**Cl**	Chlorobenzene	64	13.43
6	**9**-PF_6	Chlorobenzene	31	11.71
7	**9**-BPh_4	Chlorobenzene	22	7.95
8	**9**-NO_3	Chlorobenzene	17	12.90
9	**9**-$OCOCF_3$	Chlorobenzene	9	12.72
10	**10b**	Chlorobenzene	58	–
11	**11**	Toluene	21	–
12	**11**	Chlorobenzene	39	–

[a] The chemical shift values of NH moieties in $CDCl_3$.

somewhat superior to those in toluene as illustrated in entries 4, 5 and 11, 12. The rhodium complexes **9**-$\mathbf{PF_6}$, **9**-$\mathbf{BPh_4}$, **9**-$\mathbf{NO_3}$, and **9**-$\mathbf{OCOCF_3}$ are examined in addition to **9**-**Cl**. Among the catalysts examined, **9**-**Cl** shows the best reactivity (64% yield, entry 5). In the case of **9**-$\mathbf{BPh_4}$, where no anion-recognition is expected, the yield is significantly decreased (22%, entry 7). This means that the presence of the chloride anion near the metal center enhances activity of the catalysts in alkyne cyclotrimerization reactions. The PF_6 anion can also improve the reactivity (31% yield, entry 6), though the effect is small. In contrast, less reactivity than **9**-$\mathbf{BPh_4}$ is observed in the reactions with **9**-$\mathbf{NO_3}$ (17% yield, entry 8) and **9**-$\mathbf{OCOCF_3}$ (9% yield, entry 9). Since the anions would be placed near the metal centers in **9**-$\mathbf{NO_3}$ and **9**-$\mathbf{OCOCF_3}$, the anions disturb the catalytic reactions in these cases.

On the assumption that a rate-determining step in the rhodium-catalyzed cyclotrimerization reactions is a dimerization step of two alkyne molecules, which is suggested by theoretical studies [26], the experimental results can be rationalized as follows (Scheme 6). In the dimerization step of electron-poor DMAD, back-donation from metal to DMAD enhances the bond formation between the two alkyne molecules through enlargement of orbital overlapping. Electron donation from anion to the metal center would support such back-donation. When the reactions are carried out with **8a**-**Cl**, **8a**-$\mathbf{PF_6}$, and **8b**-**Cl**, the counter anions place far from the rhodium metal throughout the reactions and thus electron donation from the counter anions to the metal center hardly expected in the midst of the reactions (Scheme 7a). In contrast, the counter anion places near the metal center in an intermediate derived from **9**-**Cl** (Scheme 7b) and chloride anion could donate electron considerably to the metal center, which causes appreciable enhancement of the reactivity. In the case of the reaction with **9**-$\mathbf{PF_6}$, electron donation in an intermediate would be modest due to the weaker electron-donating ability of PF_6^-, which results in the moderate yield in the catalytic reaction. The interaction between the pyrrolic NH moiety and BPh_4^- is negligible and the poor yield is obtained when the reaction was carried out with **9**-$\mathbf{BPh_4}$. Whereas the interaction between NO_3^- ($OCOCF_3^-$) and pyrrolic NH moiety would be strong in **9**-$\mathbf{NO_3}$ **(9**-$\mathbf{OCOCF_3}$**)** as suggested by the ^{1}H NMR analyses, the yields are very low probably due to the weaker electron-donating abilities of nitrate and trifluoroacetate. Additionally, the steric repulsion between the counter anions and DMAD might be another important factor in the anion effect. Large anions near the metal center would inhibit coordination of DMAD to the rhodium metal. Nevertheless, the steric effect cannot explain all the experimental result (e.g. entries 6–8) and hence electronic perturbation from the counter anion to the metal center would be worth noting when one consider catalytic reactions with cationic complexes.

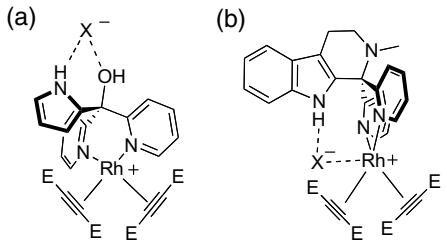

Scheme 7. Supposed structures of intermediates in rhodium catalyzed alkyne cyclotrimerization reactions.

3. Conclusion

In conclusion, the new hetero-scorpionate ligands composed of pyrrole and pyridine (**1** and **2**) and the corresponding rhodium complexes (**8**–**11**) were synthesized and characterized. In the solid state structures of **1** and **2**, varied hydrogen-bonding networks are observed depending on the steric hindrance imposed by the neighboring groups. With the cationic rhodium complexes prepared, where the counter anions are recognized by the pyrrolic NH moieties, anion effect on the rhodium-catalyzed alkyne cyclotrimerization reactions is observed. When the chloride anion places near the metal center, definite enhancement of the catalytic activity is detected. Detailed mechanistic study such as *in situ* observation of catalysts and theoretical approach to reactive species would give further important information on the alkyne cyclotrimerization reactions in the near future.

4. Experimental

All the reactions were carried out in oven-dried vessels under Ar or N_2 atmosphere. Commercially available solvents and reagents were used without further purification unless otherwise mentioned. THF was distilled over benzophenone ketyl. Thin-layer chromatography (TLC) was carried out on aluminium sheets coated with silica gel 60 (Merck5554). Preparative separations were performed by silica gel column chromatography (KANTO Silica Gel 60 N, spherical, neutral, 40–50 μm and KANTO Silica Gel 60 N, spherical, neutral, 63–210 μm). ^{1}H NMR spectra were recorded in

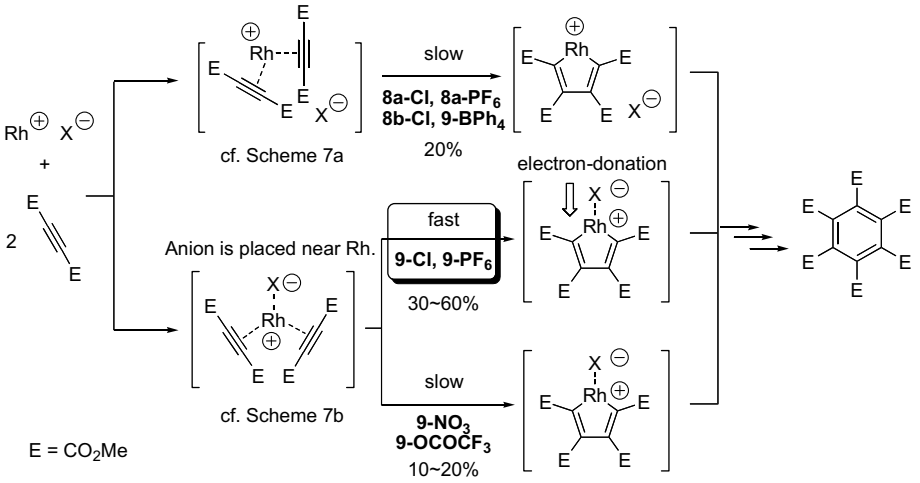

Scheme 6. Anion effect in rhodium catalyzed alkyne cyclotrimerization reactions.

$CDCl_3$ solution on a JEOL JNM-AI SERIES FT-NMR (300 MHz) spectrometer, and chemical shifts were reported relative to residual proton of deuterated solvent, $CHCl_3$ (δ = 7.26) in ppm. ^{13}C NMR spectra were recorded in $CDCl_3$ solution on the same instrument, and chemical shifts were reported relative to $CDCl_3$ (δ = 77.00) in ppm. Mass spectra were recorded on a Bruker Daltonics autoflex MALDI-TOF MS spectrometer.

4.1. Preparation of **1a**

CF_3CO_2H (150 μL, 1.95 mmol, 3.6 equiv.) was added to a mixture of pyrrole (0.36 mL, 5.4 mmol, 10 equiv.) and di-(2-pyridyl)ketone (**3**, 100 mg, 0.54 mmol, 1 equiv.) and the reaction mixture was stirred for 1 h at room temperature. After quenching by addition of Et_3N, the reaction mixture was diluted with CH_2Cl_2 and then purified by silica gel column chromatography to give **1a** in 67% yield (90 mg, 0.36 mmol, 67% yield). ^1H NMR ($CDCl_3$, 300 MHz, ppm): δ 9.41 (br s, 1H), 8.52 (dd, J = 1.5, 4.8 Hz, 2H), 7.82 (d, J = 7.8 Hz, 2H), 7.67 (dt, J = 1.5, 7.8 Hz, 2H), 7.18 (dd, J = 4.8, 7.8 Hz, 2H), 6.89 (br s, 1H), 6.77 (d, J = 1.8 Hz, 1H), 6.16 (m, 2H); ^{13}C NMR ($CDCl_3$, 75 MHz, ppm): δ 162.48, 147.47, 136.88, 134.95, 122.34, 121.65, 117.22, 108.24, 106.85, 76.39. Anal. Calc. for **1a**: C, 71.70; H, 5.21; N, 16.72. Found: C, 71.58; H, 5.24; N, 16.74%.

4.2. Preparation of **5**

To a solution of **4** (11 g, 44.7 mmol, 2.0 equiv.) in THF (140 mL), *n*-BuLi in hexane (1.6 M, 27.3 mL, 43.8 mmol, 2.0 equiv.) was added at −78 °C under an argon atmosphere. After stirring for 15 min, di-(2-pyridyl)ketone **3** (4.0 g, 21.9 mmol, 1 equiv.) was added to the reaction mixture at that temperature. The resulting solution was stirred for 1 h and then quenched with 1% CH_3CO_2H in THF. After removing the cooling bath, the reaction mixture was diluted with water and CH_2Cl_2. The organic layer was separated, washed with brine and dried over anhydrous Na_2SO_4. After filtration, the solvent was removed under reduced pressure and the residual oil was purified by silica gel column chromatography to give **5** (7.3 g, 20.8 mmol, 92% yield). While small amount of impurities were contaminated after silica gel column separation, it was used in the next step without further purification. ^1H NMR ($CDCl_3$, 300 MHz, ppm): δ 8.50 (d, J = 4.8 Hz, 2H), 7.64–7.66 (m, 4H), 7.23 (dd, J = 1.8, 3.3 Hz, 1H), 7.14 (m, 2H), 6.53 (s, 1H), 6.02 (t, J = 3.3 Hz, 1H), 5.42 (dd, J = 1.8, 3.3 Hz, 1H), 1.36 (s, 9H); ^{13}C NMR ($CDCl_3$, 75 MHz, ppm): δ 163.46, 149.82, 147.69, 138.11, 136.04, 122.91, 122.02, 121.76, 116.42, 109.47, 84.00, 78.61, 27.48; MS (MALDI, positive): m/z = 352.2 ($[MH]^+$).

4.3. Preparation of **1b**

A solution of NaOMe (3.35 g, 62 mmol, 3 equiv.) in MeOH (10 mL) was added to a solution of **5** (7.26 g, 20.7 mmol, 1 equiv.) in THF (100 mL) and stirred for 1 h at room temperature. After quenching with H_2O, and the reaction mixture was diluted with brine and CH_2Cl_2. The organic layer was separated, dried over Na_2SO_4, filtered and evaporated under reduced pressure. The residue was purified by silica gel column chromatography to give **1b** (2.21 g, 8.3 mmol, 40% yield). ^1H NMR ($CDCl_3$, 300 MHz, ppm): δ 10.78 (br s, 1H), 8.55 (dd, J = 1.8, 4.8 Hz, 2H), 7.66 (dt, J = 1.8, 8.1 Hz, 2H), 7.59 (dd, J = 0.9, 8.1 Hz, 2H), 7.14 (ddd, J = 0.9, 4.8, 8.1 Hz, 2H), 6.83 (m, 1H), 6.19 (m, 1H), 6.14 (m, 1H), 3.21 (s, 3H); ^{13}C NMR ($CDCl_3$, 75 MHz, ppm): δ 163.09, 148.28, 136.64, 131.72, 122.00, 121.91, 117.18, 109.03, 107.82, 83.50, 52.53. Anal. Calc. for **1b**: C, 72.43; H, 5.70; N, 15.84. Found: C, 72.24; H, 5.71; N, 15.94%.

4.4. Preparation of **1c**

A solution of NaOEt (1.45 g, 21 mmol, 5 equiv.) in EtOH (10 mL) was added to a solution of **5** (1.50 g, 4.2 mmol, 1 equiv.) in THF (20 mL) and stirred for 1 h at room temperature. After quenching with H_2O, and the reaction mixture was diluted with brine and CH_2Cl_2. The organic layer was separated, dried over Na_2SO_4, filtered and evaporated under reduced pressure. The residue was purified by silica gel column chromatography to give **1c** (0.53 g, 1.9 mmol, 45% yield). ^1H NMR ($CDCl_3$, 300 MHz, ppm): δ 10.78 (br s, 1H), 8.55 (dd, J = 1.8, 4.8 Hz, 2H), 7.66 (dt, J = 1.8, 8.1 Hz, 2H), 7.59 (dd, J = 0.9, 8.1 Hz, 2H), 7.14 (ddd, J = 0.9, 4.8, 8.1 Hz, 2H), 6.83 (m, 1H), 6.19 (m, 1H), 6.14 (m, 1H), 3.21 (s, 3H); ^{13}C NMR ($CDCl_3$, 75 MHz, ppm): δ 163.73, 148.24, 136.64, 132.57, 121.91, 121.70, 116.96, 108.30, 107.76, 83.03, 60.14, 15.54. Anal. Calc. for **1c**: C, 73.10; H, 6.13; N, 15.04. Found: C, 73.06; H, 6.13; N, 15.16%.

4.5. Preparation of **7**

To a solution of tryptamine (**6**) (0.87 g, 5.4 mmol, 1 equiv.) and di-(2-pyridyl)ketone (**3**) (1.0 g, 5.4 mmol, 1 equiv.) in toluene (18 mL), *p*-toluenesulfonic acid (93 mg, 0.54 mmol, 0.1 equiv.) was added and the reaction mixture was refluxed for 8 h. After cooling, the resulting mixture was quenched with aq $NaHCO_3$ and diluted with CH_2Cl_2. The organic layer was separated, dried over anhydrous Na_2SO_4, and filtered. The filtrate was concentrated under reduced pressure and the residue was purified by silica gel column chromatography to give **7** (1.35 g, 4.1 mmol, 77% yield). ^1H NMR ($CDCl_3$, 300 MHz, ppm): δ 9.51 (br s, 1H), 8.53 (d, J = 4.8 Hz, 2H), 7.65 (t, J = 4.8 Hz, 4H), 7.54 (d, J = 7.8 Hz, 1H), 7.36 (d, J = 7.8 Hz, 1H), 7.19–7.07 (m, 4H), 3.30 (br s, 1H), 3.06 (t, J = 5.4 Hz, 2H), 2.90 (t, J = 5.4 Hz, 2H); ^{13}C NMR ($CDCl_3$, 75 MHz, ppm): δ 165.00, 149.07, 136.54, 135.85, 133.62, 127.06, 121.82, 121.76, 121.72, 119.12, 118.50, 111.15, 110.31, 66.01, 40.10, 22.15. Anal. Calc. for **7**: C, 77.28; H, 5.56; N, 17.17. Found: C, 77.30; H, 5.55; N, 17.34%.

4.6. Preparation of **2**

A suspension of **7** (0.10 g, 0.31 mmol, 1 equiv.), $NaHCO_3$ (0.36 g, 4.3 mmol, 14 equiv.) and MeI (1.8 mL, 29 mmol, 90 equiv.) in MeOH (40 mL) was stirred for 2 d at room temperature. The reaction mixture was quenched with aq NH_4Cl and diluted with CH_2Cl_2. The organic layer was separated, dried over anhydrous Na_2SO_4, and filtered. The solvent was removed under reduced pressure and the residue was purified by silica gel column chromatography to give **2** (104 mg, 0.30 mmol, 99% yield). ^1H NMR ($CDCl_3$, 300 MHz, ppm): δ 8.94 (br s, 1H), 8.61 (dd, J = 1.2, 4.8 Hz, 2H), 7.63 (dt, J = 1.2, 7.8 Hz, 2H), 7.54 (d, J = 1.2, 7.2 Hz, 1H), 7.52 (dd, J = 1.2, 7.8 Hz, 2H), 7.23 (d, J = 1.2, 7.2 Hz, 1H), 7.15 (ddd, J = 1.2, 4.8, 7.8 Hz, 2H), 7.09 (dt, J = 1.2, 7.2 Hz, 2H), 2.98 (s, 4H), 2.28 (s, 3H); ^{13}C NMR ($CDCl_3$, 75 MHz, ppm): δ 161.85, 148.45, 136.26, 136.06, 134.72, 126.55, 123.44, 121.79, 121.63, 118.98, 118.41, 111.06, 109.42, 71.10, 48.12, 40.14, 21.14; MS (MALDI, positive): m/z = 340.9 ($[MH]^+$). Anal. Calc. for **2** · $0.1CH_2Cl_2$: C, 76.07; H, 5.84; N, 16.06. Found: C, 76.13; H, 5.92; N, 16.09%.

4.7. Preparation of **8a-Cl**

A solution of **1a** (50 mg, 0.20 mmol, 1 equiv.) and $[RhCl(cod)]_2$ (59 mg, 0.12 mmol, 0.6 equiv.) in CH_2Cl_2 (10 mL) was stirred for 15 min at room temperature. The solvent was removed under reduced pressure and the residue was purified by silica gel column chromatography to give **8a-Cl** (94 mg, 0.19 mmol, 95% yield). ^1H NMR ($CDCl_3$, 300 MHz, ppm): δ 11.03 (br s, 1H), 8.44 (br s, 2H),

8.28 (d, J = 7.8 Hz, 2H), 7.90 (t, J = 7.8 Hz, 2H), 7.32 (m, 3H), 7.15 (br s, 1H), 6.47 (s, 1H), 6.26 (s, 1H), 4.13 (s, 1H), 3.31 (br s, 3H), 2.37 (br s, 4H), 1.76 (br s, 4H); ^{13}C NMR ($CDCl_3$, 75 MHz, ppm): δ 161.79, 148.23, 139.14, 132.72, 125.23, 124.71, 123.83, 110.24, 107.56, 78.46, 30.92, 30.52; MS (MALDI, positive): m/z = 461.1 ([M−HCl]$^+$).

4.8. Preparation of **8b-Cl** and **10b**

A solution of **1b** (50 mg, 0.19 mmol, 1 equiv.) and $[RhCl(cod)]_2$ (56 mg, 0.11 mmol, 0.6 equiv.) in CH_2Cl_2 (10 mL) was stirred for 15 min at room temperature. The solvent was removed under reduced pressure and the residue was purified by silica gel column chromatography to give **8b-Cl** (91 mg, 0.18 mmol, 95% yield). Treatment of a CH_2Cl_2 solution of **8b-Cl** with aq $NaHCO_3$ afforded **10b** in a quantitative yield. **8b-Cl**: ^{1}H NMR ($CDCl_3$, 300 MHz, ppm): δ 11.65 (br s, 1H), 8.97 (br s, 1H), 7.89 (s, 5H), 7.35 (m, 3H), 6.41 (s, 1H), 6.31 (s, 1H), 4.04 (s, 1H), 3.66 (br s, 1H), 2.97 (s, 3H), 2.43−1.54 (m, 8H); ^{13}C NMR ($CDCl_3$, 75 MHz, ppm): δ 149.49139.40, 126.25, 125.88, 123.66, 116.10, 107.32, 84.21, 52.94, 31.55, 30.95, 27.97, 22.62, 14.10. **10b**: ^{1}H NMR ($CDCl_3$, 300 MHz, ppm): δ 8.52 (d, J = 4.8 Hz, 2H), 7.73 (m, 4H), 7.15 (m, 2H), 6.53 (s, 1H), 6.27 (s, 1H), 6.10 (s, 1H), 4.13 (br s, 2H), 3.34 (br s, 2H), 3.24 (s, 3H), 2.12−1.61 (m, 8H); ^{13}C NMR ($CDCl_3$, 75 MHz, ppm): δ 149.49, 136.74, 132.43, 125.66, 125.64, 125.08, 122.37, 106.28, 106.26, 105.98, 87.21, 81.80 (br), 79.91 (br), 53.60, 29.91. Anal. Calc. for **10b** · 0.7CH_2Cl_2: C, 55.47; H, 5.16; N, 7.86. Found: C, 55.80; H. 5.18; N, 7.85%.

4.9. Preparation of **9-Cl** and **11**

A solution of **2** (50 mg, 0.15 mmol, 1 equiv.) and $[RhCl(cod)]_2$ (45 mg, 0.091 mmol, 0.6 equiv.) in CH_2Cl_2 (10 mL) was stirred for 15 min at room temperature under an argon atmosphere. The solvent was removed under reduced pressure and the residue was purified by silica gel column chromatography to give **9-Cl** (85 mg, 0.15 mmol, 95% yield). Treatment of a CH_2Cl_2 solution of **9-Cl** with aq $NaHCO_3$ afforded **11** in a quantitative yield. **9-Cl**: ^{1}H NMR ($CDCl_3$, 300 MHz, ppm): δ 13.43 (br s, 1H), 9.11 (d, J = 7.2 Hz, 1H), 8.94 (d, J = 5.4 Hz, 1H), 8.22−8.13 (m, 3H), 7.72−7.64 (m, 2H), 7.53 (d, J = 7.2 Hz, 1H), 7.42 (d, J = 6.9 Hz, 1H), 7.13–7.36 (m, 3H), 3.86−3.80 (m, 1H), 3.70 (s, 4H), 3.07−3.29 (m, 2H), 2.81−2.57 (m, 5H), 2.43 (s, 3H), 2.09−1.95 (m, 4H); ^{13}C NMR ($CDCl_3$, 75 MHz, ppm): δ 160.57, 155.11, 149.91, 146.49, 140.44, 140.08, 137.77, 127.49, 127.07, 125.95, 125.54, 124.85, 124.24, 123.11, 119.71, 117.76, 117.68, 114.34, 108.72, 75.47 (d, J_{Rh-C} = 13.7 Hz), 75.03 (d, J_{Rh-C} = 14.3 Hz), 51.30, 38.95, 31.73, 30.61, 17.50; MS (MALDI, positive): m/z = 551 ([M–Cl]$^+$). **11**: ^{1}H NMR ($CDCl_3$, 300 MHz, ppm): δ 8.67 (d, J = 4.9 Hz, 2H), 7.82 (br s, 2H), 7.74 (dt, J = 1.4, 7.6 Hz, 2H) 7.46−7.36 (m, 2H), 7.20 (br t, J = 6.0 Hz, 2H), 6.93−6.83 (m, 2H), 3.43 (br s, 2H), 2.98 (s, 5H); ^{13}C NMR ($CDCl_3$, 75 MHz, ppm): δ 148.78, 145.26, 145.24, 138.98, 136.61, 128.93, 125.21, 121.89, 118.37, 117.38, 115.88, 114.24, 108.01, 79.24, 74.16, 53.42, 48.87, 40.98, 29.47, 22.20; Anal. Calc. for **11** · 0.8CH_2Cl_2: C, 59.72; H, 5.47; N, 9.04. Found: C, 59.95; H. 5.36; N, 9.00%.

4.10. Typical procedure for anion exchange

8-Cl or **9-Cl** in CH_2Cl_2 was treated with slightly excess amounts of AgX or NaX. After filtration and evaporation, the residue was recrystallized from CH_2Cl_2/hexane to give **8-X** or **9-X**.

4.11. Preparation of **8a-PF$_6$**

Starting from 58 mg (0.12 mmol) of **8a-Cl**, 64 mg of **8a-PF$_6$** was obtained (0.105 mmol, 88% yield). ^{1}H NMR ($CDCl_3$, 300 MHz, ppm): δ 9.28 (br s, 1H), 8.49 (d, J = 4.8 Hz, 2H), 8.25 (d, J = 7.9 Hz, 2H), 7.97 (dt, J = 1.8, 7.9 Hz, 2H), 7.38 (ddd, J = 1.2, 5.5, 7.3 Hz, 2H), 7.20 (dd, J = 2.8, 4.0 Hz, 2H), 6.38–6.34 (m, 2H), 4.15 (s, 1H), 3.70–3.47 (m, 4H), 2.41–2.30 (m, 4H), 1.82–1.74 (m, 4H).

4.12. Preparation of **9-PF$_6$**

Starting from 10 mg (17 μmol) of **9-Cl**, 10 mg of **9-PF$_6$** was obtained (14 μmol, 84% yield). ^{1}H NMR ($CDCl_3$, 300 MHz, ppm): δ 11.71 (br s, 1H), 8.97 (d, J = 4.4 Hz, 1H), 8.80 (d, J = 8.0 Hz, 1H), 8.25 (d, J = 5.1 Hz, 1H), 8.12 (dt, J = 1.0, 8.0 Hz, 1H), 8.06 (d, J = 8.0 Hz, 1H), 7.68 (t, J = 8.0 Hz, 1H), 7.55 (d, J = 7.8 Hz, 1H), 7.48 (d, J = 8.0 Hz, 1H), 7.46–7.42 (m, 1H), 7.38–7.15 (m, 3H, overlapped with the $CHCl_3$ signal), 3.82 (dd, J = 5.2, 13.2 Hz, 1H), 3.75–3.68 (m, 4H), 3.32–3.06 (m, 2H), 2.82–2.46 (m, 5H), 2.44 (s, 3H), 2.13–1.91 (m, 4H).

4.13. Preparation of **9-BPh$_4$**

Starting from 30 mg (51 μmol) of **9-Cl**, 40 mg of **9-BPh$_4$** was obtained (46 μmol, 90% yield). ^{1}H NMR ($CDCl_3$, 300 MHz, ppm): δ 11.60 (br s, 1H), 8.27 (d, J = 5.1 Hz, 1H), 7.95 (s, 1H), 7.70–7.65 (m, 1H), 7.54 (d, J = 7.6 Hz, 1H), 7.45–7.13 (m, 16H, overlapped with the $CHCl_3$ signal), 6.91–6.75 (m, 12H), 3.73–3.61 (m, 5H), 3.24–3.10 (m, 1H), 3.00–2.88 (m, 1H), 2.76–2.50 (m, 5H), 2.29 (s, 3H), 2.12–1.90 (m, 4H).

4.14. Preparation of **9-NO$_3$**

Starting from 106 mg (181 μmol) of **9-Cl**, 110 mg of **9-NO$_3$** was obtained (179 μmol, 99% yield). ^{1}H NMR ($CDCl_3$, 300 MHz, ppm): δ 12.90 (br s, 1H), 8.95 (d, J = 5.1 Hz, 1H), 8.90 (d, J = 8.1 Hz, 1H), 8.23 (d, J = 5.1 Hz, 1H), 8.12 (dt, J = 1.8, 7.8 Hz, 1H), 8.02 (d, J = 8.1 Hz, 1H), 7.70 (dt, J = 1.5, 7.8 Hz, 1H), 7.58 (d, J = 7.8 Hz, 1H), 7.55 (d, J = 8.1 Hz, 1H), 7.45–7.39 (m, 1H), 7.36–7.14 (m, 3H, overlapped with the $CHCl_3$ signal), 3.82 (dd, J = 5.4, 13.0 Hz, 1H), 3.75–3.66 (m, 4H), 3.33–3.07 (m, 2H), 2.79 (dd, J = 4.8, 13.0 Hz, 1H), 2.77–2.45 (m, 5H), 2.44 (s, 3H), 2.14–1.90 (m, 4H).

4.15. Preparation of **9-OCOCF$_3$**

Starting from 106 mg (181 μmol) of **9-Cl**, 85 mg of **9-OCOCF$_3$** was obtained (125 μmol, 69% yield). ^{1}H NMR ($CDCl_3$, 300 MHz, ppm): δ 12.72 (s, 1H), 8.97 (d, J = 4.8 Hz, 1H), 8.78 (d, J = 8.4 Hz, 1H), 8.25 (d, J = 5.1 Hz, 1H), 8.05 (dt, J = 1.8, 8.0 Hz, 1H), 7.85 (d, J = 8.0 Hz, 1H), 7.66 (dt, J = 1.5, 8.4 Hz, 1H), 7.56 (d, J = 7.7 Hz, 1H), 7.50 (d, J = 7.7 Hz, 1H), 7.43 (dd, J = 5.6, 7.4 Hz, 1H), 7.35–7.15 (m, 3H, overlapped with the $CHCl_3$ signal), 3.83 (dd, J = 5.1, 12.6 Hz, 1H), 3.76–3.69 (m, 4H), 3.33–3.07 (m, 2H), 2.80 (dd, J = 4.5, 16.2 Hz, 1H), 2.74–2.51 (m, 5H), 2.44 (s, 3H), 2.15–1.90 (m, 4H).

4.16. X-ray diffraction studies

X-ray analysis was performed on a SMART APEX equipped with CCD detector (Brucker) using Mo Kα (graphite, monochromated, λ = 0.71069 Å) radiation. Crystal data and data statistics of **1a**, **1b**, **1c**, **2**, **8a-Cl**, **8a-PF$_6$**, and **11** are summarized in Tables 5 and 6. The structures were solved by the direct method of SHELXS-97 and refined using the SHELXL-97 program [27]. The non-hydrogen atoms were refined anisotropically by the full-matrix least square method. Hydrogen atoms were refined isotropically for **1a**, **1b**, **1c**, and **2**, and were placed at calculated positions for **8a-Cl**, **8a-PF$_6$**, and **11**.

Table 5
Crystal data and structure analysis results

	La	Ib	Ic	2
Formula	$C_{15}H_{13}N_30$	$C_{16}H_{15}N_30$	$C_{17}H_{17}N_30$	$C_{22}H_{20}N_4$
Crystal system	Monoclinic	Orthorhombic	Triclinic	Monoclinic
Space group	$P2_1/c$ (No. 14)	*Pbca* (No. 61)	$P\bar{1}$ (No. 2)	$P2_1/c$ (No. 14)
R, $Rw(I > 2\sigma(I))$	0.0390, 0.0453	0.0320, 0.0476	0.0473, 0.0530	0.0400, 0.0685
R_1, wR_2 (all data)	0.1009,0.1051	0.0765, 0.0810	0.1337,0.1388	0.0831,0.0896
Goodness-of-fit	1.057	0.919	1.073	0.850
a (Å)	11.1699(19)	10.918(5)	8.6358(6)	8.5804(5)
b (Å)	8.0159(13)	14.885(6)	8.8382(6)	12.2131(7)
c (Å)	13.685(2)	16.612(7)	10.4813(7)	17.1707(10)
α (°)	90	90	95.551(2)	90
β (°)	91.249(4)	90	100.537(1)	100.226(2)
γ (°)	90	90	105.804(1)	90
V (Å^3)	1225.0(3)	2700(2)	747.63(9)	1770.79(18)
Z	4	8	2	4
T (K)	223(2)	223(2)	173(2)	223(2)
Crystal size (mm)	0.36 × 0.31 × 0.22	0.22 × 0.12 × 0.08	0.60 × 0.36 × 0.14	0.15 × 0.12 × 0.08
D_{calc} (g cm^{-3})	1.363	1.306	1.241	1.277
$2\theta_{\mu lv}$,$2\theta_{\mu\alpha\xi}$ (°)	3.6, 52.0	4.9, 50.5	4.0, 55.0	4.1,55.0
Number of reflections measured (unique)	2399	2437	3402	4074
Number of reflections measured ($I > 2\sigma(I)$)	1987	1769	2863	2541
Number of parameters	225	242	259	316
Δ (e Å^{-3})	0.241, −0.186	0.179, −0.143	0.418, −0.300	0.215, −0.215

Table 6
Crystal data and structure analysis results

	8a-Cl	8a-PF_6	11
Formula	$C_{23}H_{24}ClN_3ORh$	$C_{30}H_{31}N_4Rh \cdot 0.5CH_2Cl_2$	$2(C_{30}H_{31}N_4Rh) \cdot CH_2Cl_2$
Crystal system	Triclinic	Orthorhombic	Orthorhombic
Space group	$P\bar{1}$ (No. 2)	$Pna2_1$ (No. 33)	$Pna2_1$ (No. 33)
R, $Rw(I > 2\sigma(I))$	0.0344, 0.0377	0.0385, 0.0562	0.0326, 0.0449
R_1,wR_2 (all data)	0.0889, 0.0904	0.0755, 0.0794	0.0692, 0.0719
Goodness-of-fit	1.008	0.880	0.927
a (Å)	9.4982(5)	20.2257(10)	20.2257(10)
b (Å)	10.5132(5)	18.3289(9)	18.3289(9)
c (Å)	12.1101(6)	14.1306(7)	14.1306(7)
α (°)	95.953(1)	90	90
β (°)	106.676(1)	90	90
γ (°)	113.828(1)	90	90
V (Å^{-3})	1025.84(9)	5238.4(4)	5238.4(4)
Z	2	8	4
T (K)	223(2)	243(2)	243(2)
Crystal size (mm)	0.23 × 0.15 × 0.05	0.18 × 0.06 × 0.05	0.18 × 0.06 × 0.05
D_{calc} (g cm^{-3})	1.608	1.504	1.504
$2\theta_{\mu lv}$,$2\theta_{\mu\alpha\xi}$ (°)	3.6, 52.0	3.0, 52.0	3.0, 52.0
Number of reflections measured (unique)	4009	10,268	5379
Number of reflections measured ($I > 2\sigma(I)$)	3604	7695	4344
Number of parameters	263	660	660
Δ (e Å^3)	0.712, −0.765	0.954, −0.367	0.990, −0.360

Acknowledgements

The present work was supported by the Grant-in-Aid for Scientific Research (16350024 and 19750036) and the Global COE Program "Science for Future Molecular Systems" from the Ministry of Education, Culture, Sports, Science and Technology of Japan.

Appendix A. Supplementary material

CCDC 678429, 678430, 678431, 678432, 664292, 664293 and 664294 contain the supplementary crystallographic data for this paper. These data can be obtained free of charge from The Cambridge Crystallographic Data Centre via www.ccdc.cam.ac.uk/data_request/cif. Supplementary data associated with this article can be found, in the online version, at doi:10.1016/j.jorganchem.2008.07.005.

References

[1] S. Trofimenko, J. Am. Chem. Soc. 88 (1966) 1842.
[2] (a) S. Trofimenko, Chem. Rev. 93 (1993) 943;
(b) D.L. Roger, Coord. Chem. Rev. 147 (1996) 571;
(c) M. Etienne, Coord. Chem. Rev. 156 (1997) 201;
(d) C. Janiak, Coord. Chem. Rev. 163 (1997) 107.
[3] (a) M. Akita, J. Organomet. Chem. 689 (2004) 4540;
(b) M. Akita, S. Hikichi, Bull. Chem. Soc. Jpn. 75 (2002) 1657.
[4] (a) M. Toganoh, T. Ishizuka, H. Furuta, Chem. Commun. (2004) 2464;
(b) M. Toganoh, H. Furuta, Chem. Lett. (2005) 1034;
(c) M. Toganoh, S. Ikeda, H. Furuta, Chem. Commun. (2005) 4589;
(d) M. Toganoh, S. Ikeda, H. Furuta, Inorg. Chem. 46 (2007) 10003;
(e) M. Toganoh, K. Fujino, S. Ikeda, H. Furuta, Tetrahedron Lett. 49 (2008) 1488.
[5] A. Otero, J. Fernández-Baeza, A. Antiñolo, J. Tejeda, A. Lara-Sánchez, Dalton Trans. (2004) 1499.
[6] C. Pettinari, A. Cingolani, G. Gioia Lobbia, F. Marchetti, D. Martini, M. Pellei, R. Pettinari, C. Santini, Polyhedron 23 (2004) 451.
[7] (a) C. Janiak, J. Chem. Soc., Chem. Commun. (1994) 545;
(b) J. Reglinski, M. Garner, I.D. Cassidy, P.A. Slavin, M.D. Spicer, D.R. Armstrong, J. Chem. Soc., Dalton Trans. (1999) 2119;

(c) W. Kläui, M. Berghahn, W. Frank, G.J. Reiß, T. Schönherr, G. Rheinwald, H. Lang, Eur. J. Inorg. Chem. (2003) 2059;
(d) S.-J. Chiou, P. Ge, C.G. Riordan, L.M. Liable-Sands, A.L. Rheingold, Chem. Commun. (1999) 159;
(e) P.J. Bailey, M. Lanfranchi, L. Marchiò, S. Parsons, Inorg. Chem. 40 (2001) 5030;
(f) M. Careri, L. Elviri, M. Lanfranchi, L. Marchiò, C. Mora, M.A. Pellinghelli, Inrog. Chem. 42 (2003) 2109.
[8] (a) S. Trofimenko, J. Am. Chem. Soc. 92 (1970) 5118;
(b) V.S. Joshi, V.K. Kale, K.M. Sathe, A. Sarkar, S.S. Tavale, C.G. Soresh, Organometallics 10 (1991) 2898;
(c) C. Kimblin, V.J. Murphy, G. Parkin, J. Chem. Soc., Chem. Commun. (1996) 235;
(d) L.M. Richburg, J.A. Farouq, C.D. Incarvito, A.L. Rheingold, D. Rabinovich, Polyhedron 19 (2000) 1815.
[9] (a) J.L. Sessler, S. Camiolo, P.A. Gale, Coord. Chem. Rev. 240 (2003) 17;
(b) H. Maeda, Eur. J. Org. Chem. (2007) 5313.
[10] (a) H. Maeda, Y. Ishikawa, T. Matsuda, A. Osuka, H. Furuta, J. Am. Chem. Soc. 125 (2003) 11822;
(b) H. Maeda, T. Morimoto, A. Osuka, H. Furuta, Chem. Asian J. 1 (2006) 832;
(c) Y. Xie, T. Morimoto, H. Furuta, Angew. Chem., Int. Ed. 45 (2006) 6907.
[11] (a) H. Maeda, A. Osuka, H. Furuta, Supramol. Chem. 15 (2003) 447;
(b) T. Morimoto, H. Furuta, Supramol. Chem. 19 (2007) 493.
[12] A. Macchioni, Chem. Rev. 105 (2005) 2039.
[13] (a) P.A. Duckmanton, A.J. Blake, J.B. Love, Inorg. Chem. 44 (2005) 7708;
(b) J. van den Broeke, E. de Wolf, B.-J. Deelman, G. van Koten, Adv. Synth. Catal. 345 (2003) 625.
[14] S. Burling, L.D. Field, B.A. Messerle, P. Turner, Organometallics 23 (2004) 1714.
[15] H. Terai, H. Takaya, T. Naota, Tetrahedron Lett. 47 (2006) 1705.
[16] (a) X. Tong, Z. Zhang, X. Zhang, J. Am. Chem. Soc. 125 (2003) 6370;
(b) K. Tanaka, G.C. Fu, J. Am. Chem. Soc. 123 (2001) 11492.
[17] (a) Y. Ono, H. Furuta, Chem. Lett. 35 (2006) 750;
(b) F. Ito, T. Nagai, Y. Ono, K. Yamaguchi, H. Furuta, T. Nagamura, Chem. Phys. Lett. 435 (2007) 283.
[18] A. Borrini, P. Diversi, G. Ingrosso, A. Lucherini, G. Serra, J. Mol. Catal. 30 (1985) 181.
[19] (a) W. Chen, M.P. Cava, Tetrahedron Lett. 28 (1987) 6025;
(b) W. Chen, E.K. Stephenson, M.P. Cava, Y.A. Jackson, Org. Synth. 70 (1992) 151.
[20] I. Hasan, E.R. Marinelli, L.C. Lin, F.W. Fowler, A.B. Levy, J. Org. Chem. 41 (1976) 3668.
[21] E.D. Cox, J.M. Cook, Chem. Rev. 95 (1995) 1797.
[22] (a) J.P. Mayer, D. Bankaitis-Davis, J. Zhang, G. Beaton, K. Bjergarde, C.M. Andersen, B.A. Goodman, C.J. Herrera, Tetrahedron Lett. 37 (1996) 5633;
(b) W.-B. Yeh, M.-J. Lin, C.-M. Sun, Tetrahedron Lett. 44 (2003) 4923.
[23] G. Bringmann, D. Feineis, R. God, K. Maksimenka, J. Mühlbacher, K. Messer, M. Münchbach, K.-P. Gulden, E.-M. Peters, K. Peters, Tetrahedron 60 (2004) 8143.
[24] Inter or intramolecular hydrogen bondings could be formed in **1** and **2** in solution and cause the considerable low-field shifts from a free pyrrolic NH moiety ($\delta \sim 8.2$ ppm).
[25] In the case of **8a**-**Cl**, significant amount of a *bis*-Rh(I) complex of **1a** was obtained after treatment with base and hence the reaction was not completely reversible.
[26] (a) L. Orian, J.N.P. van Stralen, F.M. Bickelhaupt, Organometallics 26 (2007) 3816;
(b) K. Kirchner, M.J. Calhorda, R. Schmid, L.F. Veiros, J. Am. Chem. Soc. 125 (2003) 11721.
[27] G.M. Sheldrick, Program for the Solution of Crystal Structures, University of Göttingen, Göttingen, Germany, 1997.